

# UAV Relay Assisted Cooperative Jamming for Covert Communications over Rician Fading

Ran Zhang, Xinying Chen, Mingqian Liu, *Member, IEEE*, Nan Zhao, *Senior Member, IEEE*,  
Xianbin Wang, *Fellow, IEEE*, and Arumugam Nallanathan, *Fellow, IEEE*

**Abstract**—Covert communication can hide the legitimate transmission from unauthorized eavesdropping. Benefiting from the deployment flexibility, unmanned aerial vehicles (UAVs) can be utilized to enhance communication confidentiality. In this correspondence, we consider a covert communication network with the aid of a full-duplex UAV relay, which is employed to help the transmission and confuse the warden. The warden adopts a radiometer to detect the covert transmission. We first find the optimal detection threshold and calculate the minimum detection error probability. Furthermore, a closed-form expression of outage probability via UAV relaying is derived over Rician fading. Then, a power optimization problem is formulated to maximize the effective covert throughput with covertness constraint. Numerical results illustrate that the cooperative jamming can disrupt the warden, and the optimal power tradeoff can guarantee the covert transmission effectively.

**Index Terms**—Cooperative jamming, covert communication, power allocation, rician fading, UAV relaying.

## I. INTRODUCTION

With the explosive growth of wireless services, communication security has become a crucial requirement for wireless networks. Especially concealing the transmission of secret information is essential for achieving communication confidentiality. Covert communication, as an emerging security technique, can prevent the transmission from being intercepted [1]. The pioneering work by Bash *et al.* in [2] has proved the square root law that at most  $\mathcal{O}(\sqrt{n})$  bits can be transmitted over  $n$  channel uses covertly. The work by Sobers *et al.* in [3] exploited the uncertainties generated by an uninformed jammer to achieve covertness.

Recently, plenty of works have focused on the covert design for different scenarios, such as single-hop [4], [5] and two-hop networks [6], [7]. In [4], a full-duplex receiver was utilized by Shahzad *et al.* to generate artificial noise (AN) to confuse

the warden while receiving signal from the transmitter. Shu *et al.* in [5] proved that transmitting AN with fixed power can improve the performance of covert communication under finite blocklength. However, single-hop networks usually require higher transmit power to mitigate the effects of channel fading. Hu *et al.* proposed two schemes in [6] that adopt rate control or power control to help a greedy relay transmit the covert information. In [7], Sun *et al.* explored the optimal power control of relay under full-duplex and half-duplex modes to maximize the covert rate.

In order to extend the applications of wireless relaying, unmanned aerial vehicles (UAV) has been investigated as an aerial platform to achieve long-distance communications. A typical application is the UAV-assisted data delivery, and Zhang *et al.* provided a framework of proactive caching and file sharing for data dissemination in vehicle-to-everything networks [8]. Due to the mobility and flexibility, the trajectory of UAV was designed by Li *et al.* in [9] to maximize the secrecy rate. Liu *et al.* in [10] further discussed the UAV-assisted localization problem with unknown path-loss exponents. UAV can be combined with non-orthogonal multiple access (NOMA), and Li *et al.* studied the performance of UAV-aided NOMA multi-way relaying in [11]. Xiong *et al.* in [12] proposed a deep reinforcement learning approach for the UAV wireless energy and data transfer. In [13], the resource management was performed for UAV-assisted networks by Yang *et al.* via federated learning.

It is worth noting that UAV is very suitable for covert communications [14]. However, the line-of-sight (LoS) channels in UAV communications are also vulnerable to malicious wardens, and the transmission will increase the risk of detection by wardens [15]. To solve this problem, there are some studies investigating the application of UAV in covert communications [16]–[18]. In [16], a joint UAV trajectory and transmit power optimization was proposed by Zhou *et al.* to maximize the average covert transmission rate. Yan *et al.* in [17] further explored the optimal location of UAV to maximize the covert communication performance subject to a delay constraint. Chen *et al.* proposed a UAV-relayed covert communication scheme against a flying warden in [18].

However, to our best knowledge, only a few works have investigated the UAV as a relay for covert communications [18]. In addition, most of the existing works on UAV covert communications have adopted a simplified LoS channel. This motivates us to study the performance of UAV relaying in covert communication by employing more realistic and accurate Rician fading. As a consequence, this correspondence

Manuscript received December 8, 2021; revised February 11, 2022; accepted March 29, 2022. The work was supported by the National Key R&D Program of China under Grant 2020YFB1807002. The associate editor coordinating the review of this paper and approving it for publication was R. Zhang. (*Corresponding author: Nan Zhao.*)

R. Zhang, X. Chen and N. Zhao are with the Key Laboratory of Intelligent Control and Optimization for Industrial Equipment of Ministry of Education, Dalian University of Technology, Dalian 116024, P. R. China (email: zhangran.dlut@gmail.com; cxy@mail.dlut.edu.cn; zhaonan@dlut.edu.cn).

M. Liu is with the State Key Laboratory of Integrated Service Networks, Xidian University, Xi'an 710071, P. R. China. (e-mail: mqliu@mail.xidian.edu.cn)

X. Wang is with the Department of Electrical and Computer Engineering, Western University, London, ON N6A 3K7, Canada (e-mail: xianbin.wang@uwo.ca)

A. Nallanathan is with Queen Mary University of London, London, U.K. (e-mail: a.nallanathan@qmul.ac.uk).

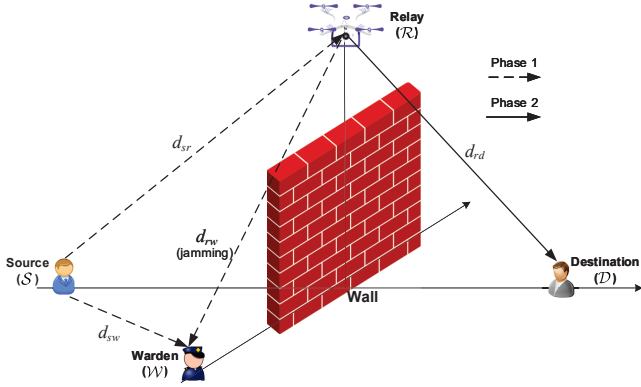


Fig. 1. UAV relaying system for covert communication.

considers a UAV relay assisted wireless network, where the full-duplex relay not only receives the signal, but also transmits AN to confuse the warden to achieve covert communication over Rician fading. The AN under this channel characteristic can effectively confuse the warden's detection.

The main contributions are summarized as follows. First, the optimal threshold of the warden and the conditions under which the warden makes detection errors are derived. Then, we present the closed-form expression of outage probability over Rician fading, and define the effective covert rate as the objective function. Finally, we present the power optimization for source and relay to maximize the covert rate subject to the covertness constraint.

## II. SYSTEM MODEL

Consider a one-way relaying system in Fig. 1, where the source ( $\mathcal{S}$ ) attempts to transmit to the destination ( $\mathcal{D}$ ) with the help of a UAV relay ( $\mathcal{R}$ ). The direct link between  $\mathcal{S}$  and  $\mathcal{D}$  is unavailable due to the blocking. The UAV is hovering with a quasi-stationary state during the whole relaying. At the same time, a warden ( $\mathcal{W}$ ) near  $\mathcal{S}$  tries to make a critical decision about whether the transmission is on or off. Assume that  $\mathcal{W}$  knows the potential time when  $\mathcal{S}$  may transmit, and it has complete knowledge about the network structure<sup>1</sup>.

All the wireless channels are assumed to undergo both large-scale path-loss and small-scale fading, and the channel coefficients between  $\mathcal{S}$ ,  $\mathcal{W}$ ,  $\mathcal{D}$  and  $\mathcal{R}$  can be modeled as

$$h_{ij} = \sqrt{\beta_{ij}} g_{ij}, \quad ij \in \{sr, rd, rw, sw\}, \quad (1)$$

where  $\beta_{ij} = \beta_0 d_{ij}^{-\alpha_{ij}}$  denotes the large-scale average channel power,  $\beta_0$  is the channel power gain at unit distance, and  $d_{ij}$  represents the distance between any two given nodes. Besides, the path-loss exponent  $\alpha_{ij}$  can be calculated by using the angle-dependent probability model as

$$\alpha_{ij} = \xi_1 (1 - P_{\text{LoS}}(\theta_{ij})) + \xi_0 = \xi_1 \left( 1 - \frac{1}{1 + a e^{-b(\theta_{ij} - a)}} \right) + \xi_0, \quad (2)$$

where  $a$  and  $b$  are determined by the environmental characteristics,  $\xi_1$  and  $\xi_0$  denote the basic path-loss coefficients, and the elevation angle  $\theta_{ij} = \arcsin(\frac{H}{d_{ij}})$ .  $H$  denotes the UAV height.

<sup>1</sup>It is a worst case assuming that  $\mathcal{W}$  has complete knowledge about the network structure, which is preferred for a robust design.

The small-scale Rician fading coefficient  $g_{ij}$  with  $\mathbb{E}[|g_{ij}|^2] = 1$  can be modeled as [19]

$$g_{ij} = \sqrt{\frac{K_{ij}}{K_{ij} + 1}} g + \sqrt{\frac{1}{K_{ij} + 1}} \tilde{g}, \quad ij \in \{sr, rd, rw\}, \quad (3)$$

where  $g$  is the deterministic line-of-sight (LoS) channel component with  $|g| = 1$ , and  $\tilde{g}$  is a zero-mean unit-variance circularly symmetric complex Gaussian (CSCG) random variable of the scattered component. The Rician factor  $K_{ij}$  is a function of the elevation angle  $\theta_{ij}$ , which can be given by

$$K_{ij} = \kappa_0 + \frac{(\kappa_{\frac{\pi}{2}} - \kappa_0) 2\theta_{ij}}{\pi}, \quad (4)$$

where  $\kappa_0$  and  $\kappa_{\frac{\pi}{2}}$  are the environment depended parameters. It can be observed that Rician fading can be reduced to Rayleigh fading when  $K = 0$ , which is used to describe the small-scale fading of terrestrial channel as  $g_{sw} \sim \mathcal{CN}(0, 1)$ . Similarly, the path-loss exponent of terrestrial link can be calculated by substituting  $\theta_{sw} = 0$  into (2).

## III. COOPERATIVE RELAYING SCHEME

Assume that  $\mathcal{R}$  is equipped with both a receive antenna and a transmit antenna, and employs the amplify-and-forward (AF) model. We propose a cooperative UAV relaying scheme where  $\mathcal{R}$  adopts the full-duplex mode for receiving and jamming in the first phase. The jamming signal can degrade the detection ability of  $\mathcal{W}$ . Then, the retransmission in the second phase enables the message of  $\mathcal{S}$  to be received at  $\mathcal{D}$  covertly.

In the first phase,  $\mathcal{S}$  chooses to transmit with a fixed power  $P_s$  or nothing, and these two events are denoted by  $H_1$  and  $H_0$ , respectively. When  $H_1$  holds,  $\mathcal{S}$  maps its messages to a sequence of  $n$  complex symbols  $\mathbf{x}_s = [x_s(1), x_s(2), \dots, x_s(n)]$ . Regardless of whether  $\mathcal{S}$  sends the messages,  $\mathcal{R}$  always transmits the jamming signal  $\mathbf{x}_j = [x_j(1), x_j(2), \dots, x_j(n)]$  to confuse  $\mathcal{W}$ , with the transmit power  $P_r$ . The symbols are assumed to be independent identically distribution (i.i.d), satisfying  $\mathbb{E}[x_s(i)x_s^\dagger(i)] = 1$  and  $\mathbb{E}[x_j(i)x_j^\dagger(i)] = 1$ , where  $i = 1, \dots, n$  represents the symbol index. It is worth noting that the self-interference generated by the full-duplex relay can be partially eliminated via the effective self-interference cancellation. The residual self-interference is denoted by  $r(i)$ , where  $r(i) \sim \mathcal{CN}(0, \xi P_r \sigma^2)$  with the factor  $0 < \xi < 1$ . Thus, the received signal at  $\mathcal{R}$  can be expressed as

$$y_r(i) = \sqrt{P_s \beta_{sr}} g_{sr} x_s(i) + r(i) + n_r(i), \quad i = 1, \dots, n, \quad (5)$$

where  $n_r(i)$  is the noise at  $\mathcal{R}$  with  $\sigma_r^2$  as its variance, i.e.,  $n_r(i) \sim \mathcal{CN}(0, \sigma_r^2)$ . For simplicity, we assume that  $\sigma_k^2 = \sigma^2$  for  $k \in \{r, w, d\}$ .

In the second phase,  $\mathcal{R}$  amplifies the received signal  $y_r(i)$  with the coefficient  $G$  when  $H_1$  holds. Automatic gain control is employed by  $\mathcal{R}$  to ensure that the transmit power is  $P_r$ , where the coefficient can be expressed as  $G = P_r / (P_s \beta_{sr} |g_{sr}|^2 + \xi P_r \sigma^2 + \sigma^2)$ . We assume that even when  $\mathcal{S}$  keeps silent,  $\mathcal{R}$  also sends the jamming signal with  $P_r$ . The jamming codebook is known at  $\mathcal{D}$ , which can be successfully decoded and removed.

### A. Requirement of Covert Communication

Since the UAV relay always transmits in Phase II, either the relayed signal or the jamming signal, we mainly focus on the testing of Phase I, and  $\mathcal{W}$  has to make a decision whether  $\mathcal{S}$  is transmitting in Phase I based on the received signal. There are two error probabilities for a detection device, i.e., miss detection  $\mathbb{P}_{\text{MD}}$  and false alarm  $\mathbb{P}_{\text{FA}}$ . Accordingly, the covert communication can be achieved when the following constraint is satisfied. For any sufficiently small constant  $\epsilon_c > 0$ , the communication scheme should ensure the probability of detection error  $\mathbb{P}_{\text{E}} \triangleq \mathbb{P}_{\text{FA}} + \mathbb{P}_{\text{MD}} \geq 1 - \epsilon_c$  as  $n$  is assumed to be infinitely large, where  $\epsilon_c$  indicates the covert communication requirement. From the perspective of  $\mathcal{W}$ , any kind of detection error made by  $\mathcal{W}$  is intolerable.

### B. Problem Formulation

In this work, we focus on maximizing the effective covert rate, which can be defined as

$$R = (1 - \mathbb{P}_{\text{out}})R_{sd}, \quad (6)$$

where  $R_{sd}$  represents the required transmission rate from  $\mathcal{S}$  to  $\mathcal{D}$ , and  $\mathbb{P}_{\text{out}}$  denotes the outage probability of the UAV relaying, which will be detailed in Section V-A.

We propose a feasible and effective power allocation scheme for the relaying system to achieve the maximal covert throughput. Assume that the total transmit power  $P_{\text{sum}} = P_s + P_r$  is fixed, and set a factor  $\rho$  to define  $P_s = \rho P_{\text{sum}}$  and  $P_r = (1 - \rho)P_{\text{sum}}$ , ( $0 < \rho < 1$ ). Moreover, we should have a constraint to guarantee covertness. Thus, the optimization problem can be formulated as

$$(P1) : \max_{\rho} (1 - \mathbb{P}_{\text{out}})R_{sd} \quad (7a)$$

$$s.t. \quad \mathbb{P}_{\text{E}} \geq 1 - \epsilon_c, \quad (7b)$$

$$0 < \rho < 1. \quad (7c)$$

## IV. PERFORMANCE ANALYSIS OF COVERTNESS

In this section, we focus on handling the covertness constraint. The expression of the detection error probability is first derived, and then we calculate the optimal detection threshold to minimize the average detection error probability under a worst-case scenario.

### A. Detection Error Probability

The signal received at  $\mathcal{W}$  for each symbol index under the hypothesis  $H_0$  and  $H_1$  can be given by

$$y_w(i) = \begin{cases} \Psi + n_w(i), & H_0 \\ \sqrt{P_s \beta_{sw}} g_{sw} x_s(i) + \Psi + n_w(i), & H_1 \end{cases} \quad (8)$$

where  $i = 1, \dots, n$ ,  $\Psi = \sqrt{P_r \beta_{rw}} g_{rw} x_j(i)$  and  $n_w(i) \sim \mathcal{CN}(0, \sigma^2)$ . Note that the codebook for the signal  $x_s$  is usually unknown at  $\mathcal{W}$ .

In order to detect the transmission from  $\mathcal{S}$ ,  $\mathcal{W}$  uses the commonly-used likelihood ratio test and adopts a radiometer to conduct the binary detection [3]. Based on (8),  $\mathcal{W}$  can take

the average received power  $P_w$  as the test statistic, and the decision rule can be expressed as

$$P_w \triangleq \frac{1}{n} \sum_{i=1}^n |y_w(i)|^2 \underset{H_0}{\overset{H_1}{\geq}} \nu, \quad (9)$$

where  $\nu$  denotes the detection threshold. Based on the strong law of large numbers, the probabilities of false alarm and miss detection at  $\mathcal{W}$  are given in the following lemma.

**Lemma 1:** Let  $\bar{\lambda}_1 = P_r \beta_{rw}$  and  $\bar{\lambda}_2 = P_s \beta_{sw}$  denote the average received signal power of the  $\mathcal{R}$ - $\mathcal{W}$  and  $\mathcal{S}$ - $\mathcal{W}$  links, respectively. Let  $c_1 = \frac{K_{rw} + 1}{\bar{\lambda}_1} - \frac{1}{\bar{\lambda}_2} > 0$  and  $c_2 = \frac{K_{rw}(K_{rw} + 1)}{c_1 \bar{\lambda}_1}$  denote the constant coefficients. Then we have

$$\mathbb{P}_{\text{FA}} = \begin{cases} 1, & \nu < \sigma^2, \\ \Gamma, & \nu \geq \sigma^2, \end{cases} \quad (10)$$

and

$$\mathbb{P}_{\text{MD}} = \begin{cases} 0, & \nu < \sigma^2, \\ 1 - \Gamma - \Theta, & \nu \geq \sigma^2, \end{cases} \quad (11)$$

where

$$\Gamma = Q_1 \left( \sqrt{2K_{rw}}, \sqrt{2(1 + K_{rw}) \frac{\nu - \sigma^2}{P_r \beta_{rw}}} \right). \quad (12)$$

$Q_1(\cdot)$  is the first order Marcum Q-function and

$$\Theta = \frac{(K_{rw} + 1)e^{c_2}}{c_1 \bar{\lambda}_1 e^{K_{rw}}} e^{-\frac{\nu - \sigma^2}{\bar{\lambda}_2}} \left( 1 - Q_1 \left( \sqrt{2c_2}, \sqrt{2c_1(\nu - \sigma^2)} \right) \right). \quad (13)$$

*Proof:* According to the decision rule (9) and the strong law of large numbers, the probability of false alarm can be computed as

$$\begin{aligned} \mathbb{P}_{\text{FA}} &= \Pr(P_w \geq \nu | H_0) = \Pr \left( P_r \beta_{rw} |g_{rw}|^2 + \sigma^2 \geq \nu | H_0 \right), \\ &\stackrel{(a)}{=} \begin{cases} 1, & \nu < \sigma^2, \\ Q_1 \left( \sqrt{2K_{rw}}, \sqrt{2(1 + K_{rw}) \frac{\nu - \sigma^2}{P_r \beta_{rw}}} \right), & \nu \geq \sigma^2, \end{cases} \end{aligned} \quad (14)$$

where (a) follows the cumulative distribution function (CDF) of  $|g_{rw}|^2$ .  $Q_1(\cdot)$  is the first-order Marcum Q-function, and  $K_{rw}$  is the Rician  $K$ -factor between  $\mathcal{R}$  and  $\mathcal{W}$ .

Similarly, the probability of miss detection can be given by as

$$\mathbb{P}_{\text{MD}} = \Pr \left( P_r \beta_{rw} |g_{rw}|^2 + P_s \beta_{sw} |g_{sw}|^2 + \sigma^2 \leq \nu \right). \quad (15)$$

Note that  $\mathbb{P}_{\text{MD}}$  involves the joint distribution of two independent random variables. Recalling the channel distribution in Section II, the random variable  $\lambda_1 = P_r \beta_{rw} |g_{rw}|^2$  follows a non-central chi-square distribution with the Rician factor  $K_{rw}$ . For convenience, we drop the subscript  $rw$  from  $K_{rw}$  to simplify the notation, and the probability density function (PDF) can be given by

$$f_{\lambda_1}(x) = \frac{K + 1}{\bar{\lambda}_1 e^K} e^{-\frac{K+1}{\bar{\lambda}_1} x} I_0 \left( 2 \sqrt{\frac{K(K+1)}{\bar{\lambda}_1} x} \right), x \geq 0, \quad (16)$$

where  $\bar{\lambda}_1 = P_r \beta_{rw}$  and  $I_0(\cdot)$  is the first-kind zero-order modified Bessel function.

The second random variable  $\lambda_2 = P_s \beta_{sw} |g_{sw}|^2$  is exponentially distributed with the PDF given by

$$f_{\lambda_2}(x) = \frac{1}{\bar{\lambda}_2} e^{-x/\bar{\lambda}_2}, x \geq 0, \quad (17)$$

where  $\bar{\lambda}_2 = P_s \beta_{sw}$ . After some algebraic manipulations, the CDF of  $\lambda_1 + \lambda_2$  can be written as

$$\begin{aligned} F_\lambda(z) &= \Pr(\lambda_1 + \lambda_2 \leq z) \\ &= \int_0^z f_{\lambda_2}(\lambda_1 + \lambda_2 \leq z | \lambda_1) f_{\lambda_1}(\lambda_1) d\lambda_1 \\ &= \int_0^z \left(1 - e^{-\frac{\lambda_1 - z}{\lambda_2}}\right) \frac{K+1}{\lambda_1 e^K} e^{-\frac{(K+1)\lambda_1}{\lambda_1}} I_0\left(2\sqrt{\frac{K(K+1)\lambda_1}{\lambda_1}}\right) d\lambda_1 \\ &= \Lambda(z) - \Theta(z), \end{aligned} \quad (18)$$

where  $\Lambda(z) = \int_0^z f_{\lambda_1}(\lambda_1) d\lambda_1 = F_{\lambda_1}(z)$ , and the terms  $\Theta$  can be represented as

$$\Theta(z) = \frac{K+1}{\lambda_1 e^K} e^{-\frac{z}{\lambda_2}} \int_0^z e^{-c_1 \lambda_1} I_0\left(2\sqrt{\frac{K(K+1)\lambda_1}{\lambda_1}}\right) d\lambda_1, \quad (19)$$

where  $c_1 = \frac{K+1}{\lambda_1} - \frac{1}{\lambda_2} > 0$ . In order to solve (19), we introduce the variable  $t^2 = c_1 \lambda_1$  and substitute  $d\lambda_1 = \frac{2t}{c_1} dt$  into (19). Then, using the specific case of the incomplete Toronto function [20, Eq. (35), Eq. (38)], we can obtain the simplified expression (13) with  $c_2 = \frac{K(K+1)}{c_1 \lambda_1}$ .

Combining (15) and (18), we can obtain  $\mathbb{P}_{\text{FA}}$  and  $\mathbb{P}_{\text{MD}}$ , which completes the proof of Lemma 1. ■

Therefore, the detection error probability  $\mathbb{P}_{\text{E}}$  at  $\mathcal{W}$  for a prescribed detection threshold  $\nu$  can be given by

$$\mathbb{P}_{\text{E}} = \begin{cases} 1, & \nu < \sigma^2, \\ 1 - \Theta, & \nu \geq \sigma^2, \end{cases} \quad (20)$$

According to  $c_1 > 0$ , we have

$$\rho > \frac{\beta_{rw}}{\beta_{rw} + \beta_{sw}(K_{rw} + 1)} = \rho_{\min}, \quad (21)$$

which indicates that the power allocation factor has a new range of  $\rho \in (\rho_{\min}, 1)$ .

### B. Optimal Decision Threshold for $\mathcal{W}$

Since  $\mathcal{W}$  aims at minimizing the detection error probability  $\mathbb{P}_{\text{E}} = \mathbb{P}_{\text{FA}} + \mathbb{P}_{\text{MD}}$ , the case of  $\nu < \sigma^2$  will never be chosen because it indicates a completely incorrect detection. Thus, the optimal detection threshold  $\nu^*$  for  $\mathcal{W}$  exists when  $\nu \geq \sigma^2$ , and can be obtained by solving  $\frac{\partial \mathbb{P}_{\text{E}}}{\partial \nu} = 0$  in the following lemma.

**Lemma 2:** The optimal threshold for the detector can be calculated as

$$\frac{1 - Q_1(\sqrt{2c_2}, \sqrt{2c_1(\nu - \sigma^2)})}{2\lambda_2 c_1 e^{c_2 + c_1(\nu - \sigma^2)}} - I_0(\sqrt{4c_1 c_2(\nu - \sigma^2)}) = 0. \quad (22)$$

*Proof:* Taking the derivative of  $\mathbb{P}_{\text{E}}$  with respect to  $\nu$  yields

$$\begin{aligned} \frac{\partial \mathbb{P}_{\text{E}}}{\partial \nu} &= \left[ \frac{1 - Q_1(\sqrt{2c_2}, \sqrt{2c_1(\nu - \sigma^2)})}{\lambda_2} + \frac{\partial Q_1(\sqrt{2c_2}, \sqrt{2c_1(\nu - \sigma^2)})}{\partial \nu} \right] \\ &\quad \times \frac{(K_{rw} + 1)e^{c_2}}{c_1 \lambda_1 e^{K_{rw}}} e^{-\frac{\nu - \sigma^2}{\lambda_2}} = 0, \end{aligned} \quad (23)$$

or equivalently

$$\frac{1 - Q_1(\sqrt{2c_2}, \sqrt{2c_1(\nu - \sigma^2)})}{\lambda_2} + \frac{\partial Q_1(\sqrt{2c_2}, \sqrt{2c_1(\nu - \sigma^2)})}{\partial \nu} = 0. \quad (24)$$

According to the derivation rules, we have

$$\frac{\partial Q_1(x, y)}{\partial y} = -ye^{-\frac{x^2 + y^2}{2}} I_0(xy), \quad (25)$$

where  $x = \sqrt{2c_2}$  and  $y = \sqrt{2c_1(\nu - \sigma^2)}$ . Then, substituting (25) into (24) yields (22). Note that the equation is also mathematically intractable. Thus, the optimal threshold  $\nu^*$  can be obtained by the bisection search. ■

Under the prescribed optimal detection threshold  $\nu^*$  obtained from Lemma 2, the minimum detection error probability at  $\mathcal{W}$  can be given by

$$\mathbb{P}_{\text{E}}^* = 1 - \frac{(K_{rw} + 1)e^{-\frac{\sigma^2 - \nu^*}{\lambda_2}}}{c_1 \lambda_1 e^{K_{rw} - c_2}} \left(1 - Q_1\left(\sqrt{2c_2}, \sqrt{c_1 \lambda_2 (\nu^* - \sigma^2)}\right)\right) \quad (26)$$

Thus, the covertness constraint can be written as  $\mathbb{P}_{\text{E}}^* \geq 1 - \epsilon_c$ . Note that it is extremely difficult to analyze the monotonicity of  $\mathbb{P}_{\text{E}}^*$ , and we provide some asymptotic cases of  $\mathbb{P}_{\text{E}}^*$  in the following remark.

**Remark 1:** First, if  $\rho \rightarrow \rho_{\min}$ ,  $c_1 \rightarrow 0$  and  $c_2 \rightarrow \infty$ . Thus, the optimal detection threshold  $\nu^*$  is infinite according to the solution of (22) and the probability of  $\mathcal{W}$  to make detection errors approaches 1. Then, as  $\rho \rightarrow 1$ , which is equivalent to the case without jamming, we can derive that  $c_1 \rightarrow \infty$  and  $c_2 \rightarrow K_{rw}$ , and the minimum detection error probability approaches 0, i.e.,  $\lim_{\rho \rightarrow 1} \mathbb{P}_{\text{E}}^* = 0$ . Moreover, we use the numerical method to observe that  $\mathbb{P}_{\text{E}}^*$  first increases, and then monotonically decreases with respect to  $\rho$ , which will be confirmed in Fig. 2.

## V. COVERT RATE MAXIMIZATION

In this section, we first derive a closed-form expression of the transmission outage probability  $\mathbb{P}_{\text{out}}$  for the UAV relaying, based on which we propose power allocation scheme to maximize the covert rate subject to the covertness constraint.

### A. Transmission Outage Probability

When  $\mathcal{S}$  transmits, the signal received at  $\mathcal{D}$  after AF relaying can be given by

$$y_d(i) = g_{rd} \sqrt{\beta_{rd} G} \left[ \sqrt{\beta_{sr} P_s} g_{sr} x_s(i) + r(i) + n_r(i) \right] + n_d(i), \quad (27)$$

After some algebraic manipulations, the equivalent instantaneous end-to-end SNR at  $\mathcal{D}$  can be written as

$$\gamma_{\text{eq}} = \frac{\gamma_{sr} \gamma_{rd}}{\gamma_{sr} + \gamma_{rd} + 1}, \quad (28)$$

where  $\gamma_{sr} = P_s \beta_{sr} |g_{sr}|^2 / (\sigma^2(1 + \xi P_r))$  and  $\gamma_{rd} = P_r \beta_{rd} |g_{rd}|^2 / \sigma^2$  represent the instantaneous received SNRs on the  $\mathcal{S}$ - $\mathcal{R}$  and  $\mathcal{R}$ - $\mathcal{D}$  links, respectively. In the noise-limited system, the outage probability is defined as the probability that the channel capacity  $C_{sd} = \log_2(1 + \gamma_{\text{eq}})$  falls below the transmission rate  $R_{sd}$ , i.e.,  $C_{sd} < R_{sd}$ . Consequently, the outage probability can be given by

$$\mathbb{P}_{\text{out}} = \Pr[\gamma_{\text{eq}} < 2^{R_{sd}} - 1] = \Pr[\gamma_{\text{eq}} < \bar{\gamma}_{sd}] = F_{\gamma_{\text{eq}}}(\bar{\gamma}_{sd}), \quad (29)$$

where  $F_{\gamma_{\text{eq}}}(\cdot)$  is the CDF of  $\gamma_{\text{eq}}$ . However, the analytical evaluation of the outage probability by using  $\gamma_{\text{eq}}$  is complicated.

To facilitate the derivation of the SNR statistics,  $\gamma_{\text{eq}}$  can be approximated by its upper bound  $\gamma_{ub}$  as [21]

$$\gamma_{\text{eq}} \leq \gamma_{ub} = \min(\gamma_{sr}, \gamma_{rd}). \quad (30)$$

Thus, a closed-form lower bound to (29) can be given by

$$\begin{aligned} \mathbb{P}_{\text{out}} &= 1 - \Pr(\gamma_{sr} > \bar{\gamma}_{sd})\Pr(\gamma_{rd} > \bar{\gamma}_{sd}) \\ &= 1 - Q_1\left(\sqrt{2K_{sr}}, \sqrt{2(K_{sr}+1)(1+\xi P_r)\bar{\gamma}_{sd}\sigma^2/(P_s\beta_{sr})}\right) \\ &\quad \times Q_1\left(\sqrt{2K_{rd}}, \sqrt{2(K_{rd}+1)\bar{\gamma}_{sd}\sigma^2/(P_r\beta_{rd})}\right). \end{aligned} \quad (31)$$

The outage probability monotonically decreases with the increasing  $P_s$  and  $P_r$ , and the total transmit power is fixed. This indicated that an optimal power allocation factor  $\rho_{OP}$  can be calculated to minimize the outage probability by using the following lemma

**Lemma 3:** The closed-form solution  $\rho_{OP}$  for minimizing outage probability can be written as

$$\left(\frac{\gamma_a}{\gamma_b}\right)^{\frac{3}{4}} \frac{K_{rd}\Xi^{\frac{1}{4}}}{K_{sr}} \left(\frac{P_r}{P_s}\right)^{\frac{7}{4}} \exp\left(\sqrt{\frac{4\gamma_a}{P_s\Xi}} - \sqrt{\frac{4\gamma_b}{P_r}} + K_{rd} - K_{sr}\right) = 1, \quad (32)$$

where  $\gamma_a = K_{sr}(K_{sr} + 1)\bar{\gamma}_{sd}\sigma^2(1 + \xi P_t)/\beta_{sr}$ ,  $\gamma_b = K_{rd}(K_{rd} + 1)\bar{\gamma}_{sd}\sigma^2/\beta_{rd}$  and  $\Xi = (1 + \xi P_t)/(1 + \xi P_r)$ .

*Proof:* Refer to the proof of Theorem 1 in [22]. ■

### B. Solution to the Optimization Problem

Note that the objective function of the optimization problem (7) is equivalent to minimizing the outage probability. After obtaining the power allocation factor  $\rho_{OP}$  according to Lemma 3, we need to further discuss the relationship between  $\rho_{OP}$  and the feasible region generated by the covertness constraint  $\mathbb{P}_{\text{E}}^* \geq 1 - \epsilon_c$ , and then derive the global optimum solution  $\rho^*$ .

According to the analysis in Remark 1, for a given  $\epsilon_c$ , the covertness constraint can derive a feasible region because the limiting value of  $\mathbb{P}_{\text{E}}^*$  is different at the two ends of  $(\rho_{\min}, 1)$ , i.e.,  $\lim_{\rho \rightarrow 1} \mathbb{P}_{\text{E}}^* < \lim_{\rho \rightarrow \rho_{\min}} \mathbb{P}_{\text{E}}^*$ . In other words, the covertness constraint can yield one feasible region of  $\rho$  to ensure the covertness, i.e.,  $\mathcal{A} = \{(\rho_{\min}, \rho_C]\}$ , where  $\rho_C$  denotes the solution to the equation  $\mathbb{P}_{\text{E}}^* = 1 - \epsilon_c$ .  $\rho_C$  corresponds to the root when the covertness constraint takes the equation, and the root can be calculated by using the bisection method. If  $\rho_{OP} \in \mathcal{A}$ , the optimal factor is  $\rho^* = \rho_{OP}$ . Otherwise, the optimal factor is  $\rho^* = \rho_C$ .

## VI. NUMERICAL RESULTS AND DISCUSSION

In this section, we present simulation results to evaluate the effectiveness of the proposed scheme under covertness constraints. Without loss of generality, we assume that  $\mathcal{S}$ ,  $\mathcal{R}$ ,  $\mathcal{W}$  and  $\mathcal{D}$  are located at  $[-200, 0, 0]$ ,  $[0, 0, 50]$ ,  $[0, -300, 0]$  and  $[200, 0, 0]$  in meters, respectively. The total transmit power  $P_{\text{sum}} = 1$  W and the required transmission rate  $R_{sd} = 1$  bit/s/Hz. The channel power gain at the unit distance is  $\beta_0 = -60$  dB, and the noise power is  $\sigma^2 = -110$  dBm. Other parameters related to the channel and environment are set to  $a = 11.95$ ,  $b = 0.14$ ,  $\xi_1 = 1$ ,  $\xi_2 = 2$ ,  $\kappa_0 = 5$  dB,  $\kappa_{\frac{\pi}{2}} = 15$  dB, and  $\xi = 0.1$ .

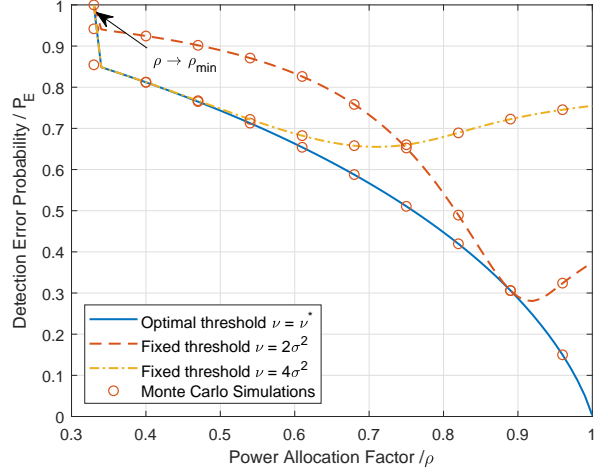


Fig. 2. Detection error probability  $\mathbb{P}_{\text{E}}$  versus the power allocation factor  $\rho$  under different detection thresholds of  $\nu = \nu^*$ ,  $\nu = 2\sigma^2$  and  $\nu = 4\sigma^2$ .

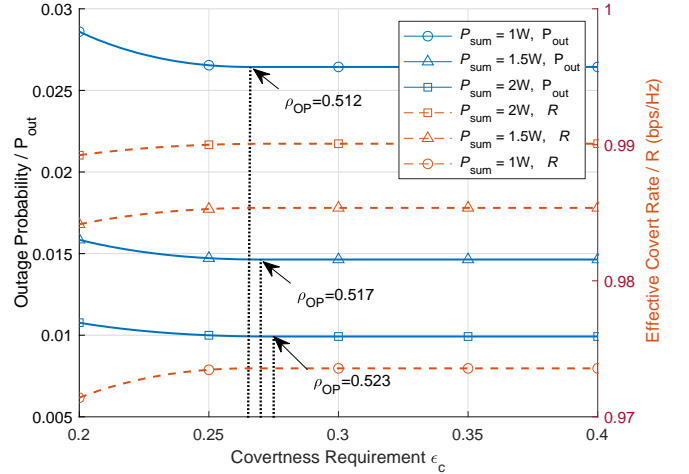


Fig. 3. Outage probability  $\mathbb{P}_{\text{out}}$  and effective covert rate  $R$  versus  $\epsilon_c$  for different  $P_{\text{sum}}$ .

Fig. 2 plots the detection error probability  $\mathbb{P}_{\text{E}}$  versus  $\rho$  for different detection thresholds. It is observed that the minimum detection error probability  $\mathbb{P}_{\text{E}}^*$  can be obtained when we have the optimal  $\nu = \nu^*$ . In addition, the fixed thresholds of  $\nu = 2\sigma^2$  and  $\nu = 4\sigma^2$  perform well when  $\rho$  is taken large and small, respectively. The Monte-Carlo results match well with the theoretical values according to (14) and (15), respectively. Furthermore, we find that an increase in  $P_j$  can create more randomness, which produces a larger detection error probability at  $\mathcal{W}$ . We also note that when  $\rho \rightarrow 1$ ,  $\mathbb{P}_{\text{E}}^*$  approaches 0, which verifies Remark 1.

Then, we show the performance of the proposed scheme in Fig. 3, which reflects the impact of covertness requirement on the objective function. It can be observed that as  $\epsilon_c$  increases,  $R$  first increases and then remains unchanged. The outage probability varies in the opposite trend to the effective covert rate. When  $\epsilon_c$  is relative small, the  $\rho_C$  calculated by the covertness constraint increases with  $\epsilon_c$ , and the maximum value of  $R$  can be directly obtained by  $\rho_C$ , leading to the

increasing of  $R$ . As  $\epsilon_c$  continues to increase, the maximum value of  $R$  can be obtained by  $\rho_{OP}$ , leading to an unchanged  $R$ . One can also see from Fig. 3 that as  $P_{\text{sum}}$  increases from 1 W to 2 W, the effective covert rate improves significantly.

## VII. CONCLUSION

In this work, we have investigated the power optimization of covert communication with the aid of a UAV relay. A cooperative relaying scheme is proposed where the full-duplex UAV relay is adopted for receiving and jamming. The goal is to maximize the effective covert throughput with the covertness constraint. We first find the optimal detection threshold of the detector and calculate the minimum detection error probability. Then, a closed-form expression of outage probability via UAV relaying is derived over Rician fading. Simulation results show that the optimal tradeoff between the information power and jamming power can be found to achieve the network covertness effectively. In the future work, we will further investigate different channel models and derive the optimal UAV location.

## REFERENCES

- [1] B. A. Bash, D. Goeckel, D. Towsley, and S. Guha, "Hiding information in noise: Fundamental limits of covert wireless communication," *IEEE Commun. Mag.*, vol. 53, no. 12, pp. 26–31, Dec. 2015.
- [2] B. A. Bash, D. Goeckel, and D. Towsley, "Limits of reliable communication with low probability of detection on AWGN channels," *IEEE J. Sel. Areas Commun.*, vol. 31, no. 9, pp. 1921–1930, Sept. 2013.
- [3] T. V. Sobers, B. A. Bash, S. Guha, D. Towsley, and D. Goeckel, "Covert communication in the presence of an uninformed jammer," *IEEE Trans. Wireless Commun.*, vol. 16, no. 9, pp. 6193–6206, Sept. 2017.
- [4] K. Shahzad, X. Zhou, S. Yan, J. Hu, F. Shu, and J. Li, "Achieving covert wireless communications using a full-duplex receiver," *IEEE Trans. Wireless Commun.*, vol. 17, no. 12, pp. 8517–8530, Dec. 2018.
- [5] F. Shu, T. Xu, J. Hu, and S. Yan, "Delay-constrained covert communications with a full-duplex receiver," *IEEE Wireless Commun. Lett.*, vol. 8, no. 3, pp. 813–816, Jun. 2019.
- [6] J. Hu, S. Yan, X. Zhou, F. Shu, J. Li, and J. Wang, "Covert communication achieved by a greedy relay in wireless networks," *IEEE Trans. Wireless Commun.*, vol. 17, no. 7, pp. 4766–4779, Jul. 2018.
- [7] R. Sun, B. Yang, S. Ma, Y. Shen, and X. Jiang, "Covert rate maximization in wireless full-duplex relaying systems with power control," *IEEE Trans. Commun.*, vol. 69, no. 9, pp. 6198–6212, Sept. 2021.
- [8] R. Zhang, R. Lu, X. Cheng, N. Wang, and L. Yang, "A UAV-enabled data dissemination protocol with proactive caching and file sharing in V2X networks," *IEEE Trans. Commun.*, vol. 69, no. 6, pp. 3930–3942, Jun. 2021.
- [9] Y. Li, R. Zhang, J. Zhang, and L. Yang, "Cooperative jamming via spectrum sharing for secure UAV communications," *IEEE Wireless Commun. Lett.*, vol. 9, no. 3, pp. 326–330, Mar. 2020.
- [10] B. Liu, X. Zhu, Y. Jiang, Z. Wei, and Y. Huang, "UAV and piecewise convex approximation assisted localization with unknown path loss exponents," *IEEE Trans. Veh. Technol.*, vol. 68, no. 12, pp. 12396–12400, Dec. 2019.
- [11] X. Li, Q. Wang, Y. Liu, T. A. Tsiftsis, Z. Ding, and A. Nallanathan, "UAV-aided multi-way NOMA networks with residual hardware impairments," *IEEE Wireless Commun. Lett.*, vol. 9, no. 9, pp. 1538–1542, Sept. 2020.
- [12] Z. Xiong, Y. Zhang, W. Y. B. Lim, J. Kang, D. Niyato, C. Leung, and C. Miao, "UAV-assisted wireless energy and data transfer with deep reinforcement learning," *IEEE Trans. Cogn. Commun. Netw.*, vol. 7, no. 1, pp. 85–99, Mar. 2021.
- [13] H. Yang, J. Zhao, Z. Xiong, K.-Y. Lam, S. Sun, and L. Xiao, "Privacy-preserving federated learning for UAV-enabled networks: Learning-based joint scheduling and resource management," *IEEE J. Sel. Areas Commun.*, vol. 39, no. 10, pp. 3144–3159, 2021.
- [14] X. Chen, N. Zhang, J. Tang, M. Liu, N. Zhao, and D. Niyato, "UAV-aided covert communication with a multi-antenna jammer," *IEEE Trans. Veh. Technol.*, vol. 70, no. 11, pp. 11619–11631, Nov. 2021.
- [15] X. Jiang, X. Chen, J. Tang, N. Zhao, X. Y. Zhang, D. Niyato, and K.-K. Wong, "Covert communication in UAV-assisted air-ground networks," *IEEE Wireless Commun.*, vol. 28, no. 4, pp. 190–197, Aug. 2021.
- [16] X. Zhou, S. Yan, J. Hu, J. Sun, J. Li, and F. Shu, "Joint optimization of a UAV's trajectory and transmit power for covert communications," *IEEE Trans. Signal Process.*, vol. 67, no. 16, pp. 4276–4290, Aug. 2019.
- [17] S. Yan, S. V. Hanly, and I. B. Collings, "Optimal transmit power and flying location for UAV covert wireless communications," *IEEE J. Sel. Areas Commun.*, vol. 39, no. 11, pp. 3321–3333, Nov. 2021.
- [18] X. Chen, M. Sheng, N. Zhao, W. Xu, and D. Niyato, "UAV-relayed covert communication towards a flying warden," *IEEE Trans. Commun.*, vol. 69, no. 11, pp. 7659–7672, Nov. 2021.
- [19] C. You and R. Zhang, "3D trajectory optimization in rician fading for UAV-enabled data harvesting," *IEEE Trans. Wireless Commun.*, vol. 18, no. 6, pp. 3192–3207, Jun. 2019.
- [20] P. C. Sofotasios, T. A. Tsiftsis, Y. A. Brychkov, S. Freear, M. Valkama, and G. K. Karagiannidis, "Analytic expressions and bounds for special functions and applications in communication theory," *IEEE Trans. on Inf. Theory*, vol. 60, no. 12, pp. 7798–7823, Dec. 2014.
- [21] H. A. Suraweera, R. H. Louie, Y. Li, G. K. Karagiannidis, and B. Vucetic, "Two hop amplify-and-forward transmission in mixed rayleigh and rician fading channels," *IEEE Commun. Lett.*, vol. 13, no. 4, pp. 227–229, Apr. 2009.
- [22] H. Tu, J. Zhu, and Y. Zou, "Optimal power allocation for minimizing outage probability of UAV relay communications," in *11th Int. Conf. Wireless Commun. Signal Process*, pp. 1–6, Oct. 2019.